Available online at BCREC website: https://bcrec.id

Bulletin of Chemical Reaction Engineering & Catalysis, 18 (1) 2023, 85-102

Research Article

Kinetics of In-Situ Catalytic Pyrolysis of Rice Husk Pellets Using a Multi-Component Kinetics Model

Wusana Agung Wibowo[1,2], Rochim Bakti Cahyono[2], R. Rochmadi[2], Arief Budiman[2,*]

[1]*Chemical Engineering Department, Universitas Sebelas Maret, Jl. Ir. Sutami 36A, Surakarta 57126, Indonesia.*
[2]*Chemical Engineering Department, Universitas Gadjah Mada, Jl. Grafika 2, Yogyakarta 55284, Indonesia.*

Received: 23rd January 2023; Revised: 22nd February 2023; Accepted: 23rd February 2023
Available online: 2nd March 2023; Published regularly: March 2023

Abstract

Ash-based catalysts, as low-cost materials, are applicable in biomass pyrolysis and play a role in lowering the activation energy. This study enriched the insights of different method of catalyst addition into biomass in the catalytic pyrolysis. The addition of rice husk ash as a catalyst into rice husk pellets allows for better solid-solid contact between the biomass and the catalyst, since the common methods were only solid mixing. This research aimed to investigate the thermal characteristics and kinetics of the biomass components (hemicellulose, cellulose, lignin) in the in-situ catalytic pyrolysis of rice husk pellets with the addition of husk ash. The three-independent parallel reaction kinetics model was used to calculate the kinetics parameters based on thermogravimetric analysis conducted at 303-873 K with various heating rates (5, 10, 20 K/min) and ash addition ratios (10:0, 10:1, 10:2). The thermogram shows that the pyrolysis of rice husk pellets was divided into two stages. Stage 1, ranging from 510-650 K, represented the decomposition of hemicellulose and cellulose, occurring faster with high mass loss, while Stage 2, starting at around 650 K, represented lignin decomposition, occurring more slowly with low mass loss. The catalytic activity of the ash was only apparent at high temperatures, where cellulose and lignin decomposition were more dominant. Activation energy, as a representation of catalytic activity for each component, was not always lower in catalytic pyrolysis. However, the average activation energy decreased with increasing heating rates and ash addition ratios. The addition of the catalyst slowed the decomposition of hemicellulose but accelerated the decomposition of cellulose and lignin.

Keywords: In-Situ Catalytic Pyrolysis; Rice Husk Ash; Thermogravimetric Analysis; Independent Parallel Reaction; Activation Energy

How to Cite: W.A. Wibowo, R.B. Cahyono, R. Rochmadi, A. Budiman (2023). Kinetics of In-Situ Catalytic Pyrolysis of Rice Husk Pellets Using a Multi-Component Kinetics Model. *Bulletin of Chemical Reaction Engineering & Catalysis*, 18(1), 85-102 (doi: 10.9767/bcrec.17226)

Permalink/DOI: https://doi.org/10.9767/bcrec.17226

1. Introduction

Rice husk is a solid waste of the rice milling industry, constituting approximately 20% of milled dry grain, thus readily available in Indonesia as an agrarian country. According to BPS statistics, in 2020, Indonesia produced 10,929,840 tons of milled dry grain, with the amount of rice husk accounting for 2.2 million tons, approximately. Despite its abundance, rice husk is still employed in modest amounts as brick- and tile-burning materials, planting medium, husk ash, husk charcoal, building materials, and adsorbents. In the chemical industry, it is applicable more efficiently using pyrolysis technology, which converts them into energy and value-added chemicals [1].

* Corresponding Author.
Email: abudiman@ugm.ac.id (A. Budiman)

Currently, the advancement of pyrolysis technology leads to the employment of selected catalysts that can boost the yields and quality of pyrolysis products. Catalysts can speed up the tar breakdown process, increasing the quantity of gas yielded [2,3]. Metal-based catalysts such as Ni, Fe, Cu, Zn, and Co are commonly employed in biomass pyrolysis [4,5]. Metal catalysts, particularly Ni, are extremely effective in increasing gas and H_2 production. Furthermore, mineral-based catalysts, such as zeolites, silica-alumina, dolomite [6], olivine, CaO, $CaCO_3$ [7], MgO, and $MgCO_3$ [8,9], are frequently employed directly and help to improve liquid product quality, reduce tar, and increase CO content.

Biomass-ash-based catalysts, which are inexpensive, can also be used in the pyrolysis process. Rice husk ash, containing high amount of silica and having a large mesoporous surface area, can be added to rice husk and has the catalytic effect of decreasing the activation energy of pyrolysis [3,10]. It can also improve the yields and quality of liquid products [11]. Rice husk ash, containing amorphous SiO_2 with high reactivity, can be obtained through controlled combustion of rice husk. The optimum temperature to obtain such superior characteristics can be reached through burning at 773 K for 12 hours. Furthermore, the SiO_2 content in rice husk ash can reach 94–96% with little K_2O, Na_2O, and Fe_2O_3 [12].

Furthermore, kinetics studies of in-situ biomass catalytic pyrolysis reactions need to be conducted to establish a reference for pyrolysis reactor design and process optimization. A wide variety of pyrolysis reaction mechanisms, ranging from the assumption that biomass can be represented by one component to that it can be represented by many components, have been proposed. In general, modeling pyrolysis reactions with a one-component global model often fails to describe the entire biomass decomposition process [13]. In terms of reaction steps, biomass pyrolysis occurs as a single-step or a multiple-step reaction. The complexity of a biomass pyrolysis reaction causes the use of the one-component-one-step reaction model in general cannot accurately represent the pyrolysis reaction [14]. Therefore, a review of more complex models that can represent biomass catalytic pyrolysis reaction mechanisms is needed.

Although the kinetics of biomass pyrolysis is extremely complex, the Independent Parallel Reaction (IPR) model is one of the best models for describing such complexities [14-18]. It properly models the pyrolysis reaction of the biomass primary components (hemicellulose, cellulose, and lignin) and generates consistent kinetic parameters with minor errors. At separate and overlapping temperature ranges, each of these biomass components thermally decomposes; hemicellulose does at 473-623 K, cellulose at 513-663 K, and lignin at 473-773 K [19,20].

Previous studies investigated biomass catalytic pyrolysis kinetics by mechanically mixing the biomass feedstock and the catalyst [21-24] or by separating from each other, but still, within one reactor [25,26]. The latter method lets the biomass pyrolyzed non-catalytically early in first stage and, further, lets the resulting volatile compounds decomposed on the catalyst surface, while the former method allows direct contact between the biomass and the catalyst. However, both methods are likely to have similar reaction mechanisms.

The addition of a catalyst to the rice husk pellets allows for better solid-solid contact between the catalyst and biomass and is expected to have a direct effect on the decomposition of each component. In this term, a few researcher focus on adding ash as a catalyst to rice husk pellets in the pyrolysis process. Therefore, this research is focused to investigate the thermal characteristics and decomposition kinetics of hemicellulose, cellulose, and lignin in the in-situ catalytic pyrolysis of rice husk pellets using husk ash as the catalyst. In this research, the thermogravimetric analysis method was used to obtain data on sample mass loss and reaction temperature as a function of time. Thermogravimetric Analysis (TGA) of non-catalytic and catalytic pyrolysis of rice husk pellets was carried out at various heating rates and ash addition ratios. The kinetics parameters were then determined with the three-independent parallel reaction (3-IPR) kinetics model representing hemicellulose, cellulose, and lignin, respectively.

2. Materials and Methods

2.1 Materials

The rice husk used was obtained from a rice milling industry in Sukoharjo, Central Java, Indonesia, in its natural and sun-dried state. It was then made into powders sized 180–250 μm before pelletization. Chemical characterization of rice husk powder was carried out through analyses of proximate, ultimate, and calorific value. The analyses were done using TA Instrument Q500, varioMICRO, and IKA C2000 basic, respectively. The analysis of biomass components was also conducted to obtain the

content of hemicellulose, cellulose, and lignin in rice husk.

2.2 Catalyst Preparation

The rice husk ash used as catalyst directly, without additional treatment, was obtained by controlled combustion of rice husk powder in a muffle furnace at 1073 K for 60 min. The ash was then placed in a desiccator until it reached ambient temperature. Re-sieving of the ash was done to obtain a size of 180–250 μm to match the size of the rice husk powder. The characterization of the husk ash was carried out through crystal phase analysis with the X-Ray Diffraction (XRD) analyzer MD10 mini-diffractometer-MTI, and the surface topography and element content analyses were done using the Scanning Electron Microscopy-Energy Dispersive X-Ray (SEM-EDX) analyzer JEOL Benchtop SEM JCM7000.

2.3 Rice Husk Pellets

Rice husk (RH) powder and rice husk ash (RHA) catalyst powder of the same size were mixed with each other at mass ratios of RH:RHA of 10:0, 10:1, and 10:2, which were then coded as RRH, ARH10, and ARH20, respectively. Each of these mixtures was then made into pellets using a 3 mm diameter pellet mold by hydraulic pressing at a tonnage of 1 ton for 5 minutes. In this study, no binder was used in the pellet production, it is intended to avoid the presence of compounds other than those contained naturally in rice husk which may affect the pyrolysis kinetics. The pelletization procedure was sufficient to maintain a good husk-ash pellets compaction for experimental purposes. The density of the pellets was then calculated based on diameter and length measurements using a standard srew micrometer, while the mass was measured using a Joanlab FA2204 analytical balance with an accuracy of 0.0001 g.

2.4 Thermogravimetric Analysis

The pyrolysis of the pellets RRH, ARH10, and ARH20 was carried out using the Thermogravimetric-Differential Scanning Calorimetry (TGA-DSC) Analyzer Linseis STA PT1000 at three constant heating rates of 5, 10, and 20 K/min. The sample rice husk pellets with 3.21 mm in diameter, weighing about 20-30 g, were placed into a ceramic cup (volume 0.12 mL) and purged with a flow of N_2 gas at 50 mL/min for 30 min to remove the oxidizer. Then the sample was heated from 303 K to 873 K in an N_2 atmosphere at a certain rate. For heating refinement, the final sample temperature was kept constant at 873 K for approximately 10 min. The sample pellets analyzed at different heating rates were then designated as shown in Table 1. The last number after the dash indicates the heating rate used.

The obtained sample mass loss data as a function of time was then processed into the Thermo Gravimetry (TG) curves or the mass fraction of residual solids (w) curves and the Differential Thermo Gravimetry (DTG) curves or the mass loss rate ($-dw/dt$) curves. The data included the start of the pyrolysis until the final temperature without involving the drying stage. The amount of the catalyst added was also not involved in the calculation of the mass fraction of residual solids. Thus, the calculation of the mass fraction of residual solids as a function of time or temperature used a catalyst-free dry basis.

2.5 Kinetics Model - the Three-Independent Parallel Reaction (3-IPR)

The one-component global reaction model has been known not to represent the results of pyrolysis data with TGA well, while the multi-component and multi-reaction models are quite good at it [14]. A widely used multi-component model is the three-independent parallel reaction (3-IPR) model, which assumes that there are three main components of biomass: hemicellulose, cellulose, and lignin. This kinetics model is useful in analyzing the effect of thermal decomposition on individual components of biomass [15,16]. Each component is considered to react separately and respectively produce volatiles and char, following the first-order or nth-order reaction [18,21]. The reaction equations for the components of biomass are as follows:

$$c_{hc0}.Hemicellulose \xrightarrow{khc} \left(c_{hc0} - v_{hc\infty}\right) Residue_{hc} + v_{hc\infty} Volatiles_{hc} \quad (1)$$

Table 1. Designation of the experiment runs.

Mass ratio of RH : RHA	Heating rate (K/min)	Sample designation
10 : 0	5	RRH-5
	10	RRH-10
	20	RRH-20
10 : 1	5	ARH10-5
	10	ARH10-10
	20	ARH10-20
10 : 2	5	ARH20-5
	10	ARH20-10
	20	ARH20-20

$$c_{cel0}.Cellulose \xrightarrow{kcel} \left(c_{cel0} - v_{cel\infty}\right) Residue_{cel} + v_{cel\infty} Volatiles_{cel} \quad (2)$$

$$c_{lig0}.Lignin \xrightarrow{klig} \left(c_{lig0} - v_{lig\infty}\right) Residue_{lig} + v_{lig\infty} Volatiles_{lig} \quad (3)$$

In the equations, $Volatiles_i$ represents the gas and condensable volatiles or tar produced from the decomposition of the component i (i = hemicellulose, cellulose, and lignin), while $Residue_i$ represents the char produced from each component i. The parameter $v_{i\infty}$ is the yield coefficient of the volatiles, while the parameter ($c_{i0} - v_{i\infty}$) is the yield coefficient of the residue. Moreover, the parameter c_{i0} represents the initial mass fraction or contribution fraction of each component in thermal decomposition of biomass [18].

The conversion of the component i (α_i) is defined as a ratio of the mass fractions of the solids reacting over time ($c_{i0} - w_{Si}$) to the initial mass fraction of the component i. w_{Si} is the mass fraction of residual solids at various times.

$$\alpha_i = \frac{\left(c_{i0} - w_{Si}\right)}{c_{i0}} \quad (4)$$

Furthermore, the decomposition kinetics of the component i can be written as follows:

$$-\frac{d\left(w_{Si}/c_{i0}\right)}{dt} = \frac{d\alpha_i}{dt} = k_i\left(1-\alpha_i\right)^{n_i} \quad (5)$$

in which k_i is the reaction rate constant and n_i is the reaction order. In this study, the first order reaction was applied to each component ($n_{hc} = n_{cel} = n_{lig} = 1$). Furthermore, the Arrhenius equation is used to define the reaction rate constant i, k_i. Eq. (5) can then be written as follows:

$$\frac{d\alpha_i}{dt} = A_i.e^{-\frac{Ea_i}{RT}}.\left(1-\alpha_i\right) \quad (6)$$

The parameter A_i is the pre-exponential factor (1/min), and Ea_i is the apparent activation energy (kJ/mol) for the component i. At constant heating rate (β=dT/dt), the kinetic equation for the reaction of the component i can be written as follows:

$$\frac{d\alpha_i}{dT} = \frac{A_i}{\beta}.e^{-\frac{Ea_i}{RT}}.\left(1-\alpha_i\right) \quad (7)$$

The calculation of the conversion α_i in the previous differential equation is carried out using the Euler method [18]. Then, the residual solid fraction based on the model (w_S^{hit}) and the sample mass loss rate over time (dw_S^{hit}/dt) are determined as follows:

$$w_S^{hit} = 1 - c_{undecomp,0} - \sum_i c_{i0}\alpha_i \quad (8)$$

$$-\frac{dw_S^{hit}}{dt} = \sum_i c_{i0}\frac{d\alpha_i}{dt} \quad (9)$$

In the previous equations, $c_{undecomp.0}$ is the mass fraction of raw materials that are not decomposed in the pyrolysis process, including char and the catalyst. The value of dα_i/dt in Equation (9) is calculated by the finite difference method. Furthermore, optimization of an objective function (OF) is carried out to obtain the values of the kinetic parameters based on initial guesses by minimizing the sum of the squared errors between the calculation results and the experimental data as follows [16,17,27]:

$$OF = \sum_{j=1}^{J}\left(\left(\frac{dw_S^{\exp}}{dt}\right) - \left(\frac{dw_S^{hit}}{dt}\right)\right)^2 \quad (10)$$

in which J is the data points (in the range of 1000-1600). Optimization is performed using the differential evolution method, which has advantages in terms of accuracy, efficiency, and reliability for complex and highly nonlinear objective function optimization. Key control parameters in the DE algorithm include NP (population size), CR (cross over constant), and F (scaling factor). Guidance for selecting the values of each of these control parameters can be found in many references [28-31]. This study used the parameter values NP = 10xN; CR = 0.9; F = 0.5, where N represents the number of kinetic parameters, which was 9 ((N = (3xA_i)+(3xEa_i)+(3xc_{i0})). The initial guess values of the kinetic parameters used in this study were based on the results of previous researchers [14-17,21]. The optimization was conducted by MATLAB R2021a software and the source code of optimization by differential evolution method was created by Wang [32]. Furthermore, validation of the kinetics model uses two references [27], namely the coefficient of determination (R^2) and fitness (Fit(%)). In this study, the model was considered valid when the R^2 value > 0.95 and the Fit(%) value < 5%.

$$R^2 = 1 - \frac{\sum_{j=1}^{J}\left(\left(\frac{dw_S^{\exp}}{dt}\right) - \left(\frac{dw_S^{hit}}{dt}\right)\right)^2}{\sum_{j=1}^{J}\left(\left(\frac{dw_S^{\exp}}{dt}\right) - \left(\frac{dw_S^{\exp}}{dt}\right)_{avg}\right)^2} \quad (11)$$

$$Fit(\%) = 100\frac{\sqrt{OF/J}}{\left(\frac{dw_S^{\exp}}{dt}\right)_{\max}} \quad (12)$$

2.6 Pyrolysis Number and Biot Number

The control regime can be determined by comparing the rate of kinetics of the pyrolysis reaction with the internal resistance to heat penetration (conduction) and external resistance to heat transfer (convection) using the group of dimensionless numbers, the pyrolysis number (*Py*) and the Biot number (*Bi*). The Py^{I} number is the ratio between the reaction rate and the internal internal resistance to heat penetration, while Py^{II} is the ratio between the reaction rate and external resistance to heat transfer. Meanwhile, *Bi* is the ratio between the internal resistance to heat penetration with external resistance to heat transfer [33].

$$Py^{I} = \frac{\lambda}{\rho.C_p.L^2.k} \quad (13)$$

$$Py^{II} = \frac{h}{\rho.C_p.L.k} \quad (14)$$

$$Bi = \frac{h.L}{\lambda} \quad (15)$$

In the equations above, the parameters h, λ, ρ, C_p, L, and k are the convective heat transfer coefficient between the hot surface and the biomass sample, the thermal conductivity of the sample, the density of the sample, the heat capacity of the sample, the characteristic length of the sample (for a cylindrical shape it can be thought of as the radius), and the reaction rate constant. For $Bi << 0.1$, the temperature throughout the solid particles were approximated to be uniform. Meanwhile, the intermediate *Bi* number (0.2-1.0) are suitable for fluidized bed pyrolysis of biomass particles. Moreover, when $Bi > 1.0$, the heat transfer is more complicated due to transient heat conduction within the particles [3].

The plot between the pyrolysis number (*Py*) and the Biot number (*Bi*) at various temperatures will produce four regions: (i) isothermal & kinetically-limited region where the entire solid part of the sample has a uniform temperature; (ii) kinetically-limited non-isothermal region, where the sample can reach the reaction temperature quickly, but with a wide temperature gradient in the solid sample; (iii) convection-limited region, where the heat transfer resistance between the heat source surface and the sample surface is dominant; and (iv) conduction-limited region, where resistance to heat conduction in solid sample is dominant [33].

3. Results and Discussion

3.1 Physico-chemical Charactheristics of Rice Husk

The rice husk pellets has a density ranging from 1.019 to 1.075 g/cm^3 with a ratio of length to diameter between 1.02 and 1.07. The proximate analysis of rice husk powder showed that the moisturize, volatile compounds, ash, and fixed carbon contents were 9.58%, 58.26%, 18.26%, and 14.00% on an air dried basis weight percentage, respectively. Meanwhile, the ultimate analysis showed that the ele-

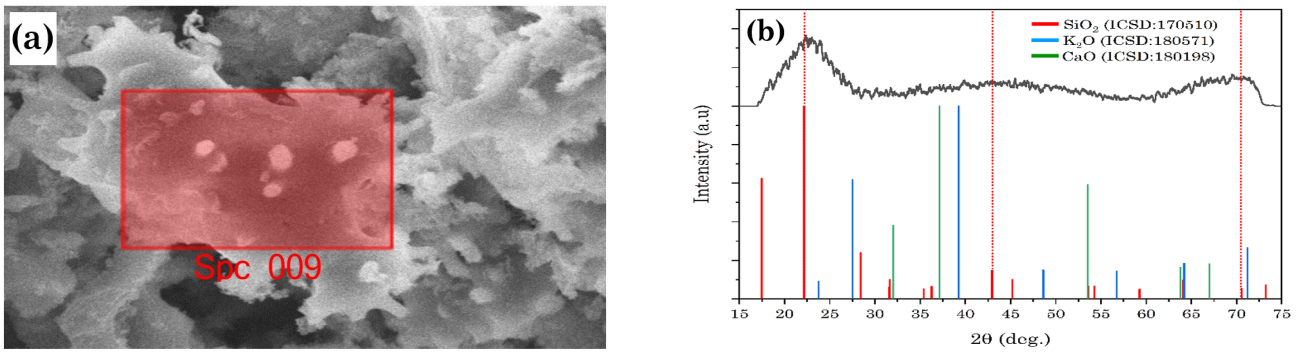

Figure 1. (a) SEM-EDX image at 5000x magnification, and (b) XRD-pattern at λ Cu Kα=1.564 Å [10].

Table 2. The composition of hemicellulose, cellulose, and lignin in rice husk.

Component	This study (% air dried basis)			Other study [35] (% air dried basis)			
	Data-1	Data-2	Avg	Reff-1	Reff-2	Reff-3	Reff-4
Hemicellulose	15.4	17.5	16.5	21	24	18	19
Cellulose	35.5	36.7	36.1	40	38	37	40
Lignin	16.9	16.6	16.8	22	19	12	16
Others	32.2	29.2	30.7	17	19	33	25

mental contents C, H, N, O, and S reached 35.24%, 5.23%, 0.33%, 40.97%, and 0.066%, respectively. The rice husk powder's higher heating value (HHV) was found to be 14.01 MJ/kg, thus potential to be used as a raw material for pyrolysis. The results of the analyses were consistent with those of previous studies [3,34]. Besides that, the amount of hemicellulose, cellulose, and lignin in rice husk and the comparation from other studies are presented in Table 2. More complete information regarding the characterizations of rice husk can be seen in our previous report [10].

3.2 Ash Characterization

The elemental analysis of the ash using SEM-EDX provided an image as shown in Figure 1(a). The rice husk ash contained a lot of Si and O with mass percentages of 45.0% and 43.4%, respectively, and little K and Ca about 1.8% and 0.3%, respectively. Carbon (C) was also found at 9.5%, which assumably was the remaining char that had not been converted during combustion. The high amounts of Si and O was thought to be related to the high amount of SiO_2 (about 90%) in the ash. The elements K and Ca could be in the form of oxides (K_2O and CaO), which have a catalytic effect and encourage the production of H_2 and CO_2 but inhibit the production of CO, CH_4, C_2H_4 and C_2H_6 [36-38].

The crystalline structure of the ash dominated by silica (SiO_2) was analyzed using XRD (Figure 1(b)), which showed that the ash had an amorphous silica structure with a crystallinity index of 30% [10]. This structure could increase the surface area of the ash. According to Shen [39], the high content of amorphous silica in rice husk ash contributes to CO_2 adsorption and increases the hydrogen-rich gas yielded. More detailed information regarding the characterization of the ash can be seen in our previous report [10].

3.3 Thermogravimetric Analysis

The characteristics of rice husk pellet thermal decomposition both in non-catalytic and catalytic pyrolysis processes were studied using TGA. Figure 2(a-f) show the results of the residual solid mass fraction curve (w or TG in %) and the mass loss rate curve ($-dw/dt$ or DTG - in %/min) based on the experiments at various heating rates and ash addition ratios. Based on the characterization of the thermal decomposition curves of TG and DTG in Figure 2(a-f), the non-catalytic and catalytic pyrolysis of rice husk pellets is divided into two stages. The first stage (Stage 1) starts at a temperature between 510-530 K and ends at a temperature between 600-650 K; there is a significant mass loss. Meanwhile, in the second stage (Stage 2) starting at 650 K until the final temperature of pyrolysis, there is a relatively gentle mass loss. The percentage of mass loss at each stage and that of residue solids for the experimental data are presented in Table 3 (Data column).

Depend on the heating rate, hemicellulose and cellulose decomposition occurs in the Stage 1 with the temperature range of 510-650 K. Meanwhile, lignin decomposition mostly does in the Stage 2 with the wider temperature range start at temperature below 650 K to final pyrolysis temperature. The temperature range of components decomposition are in accordance to previous study [40], that is, devolatilization

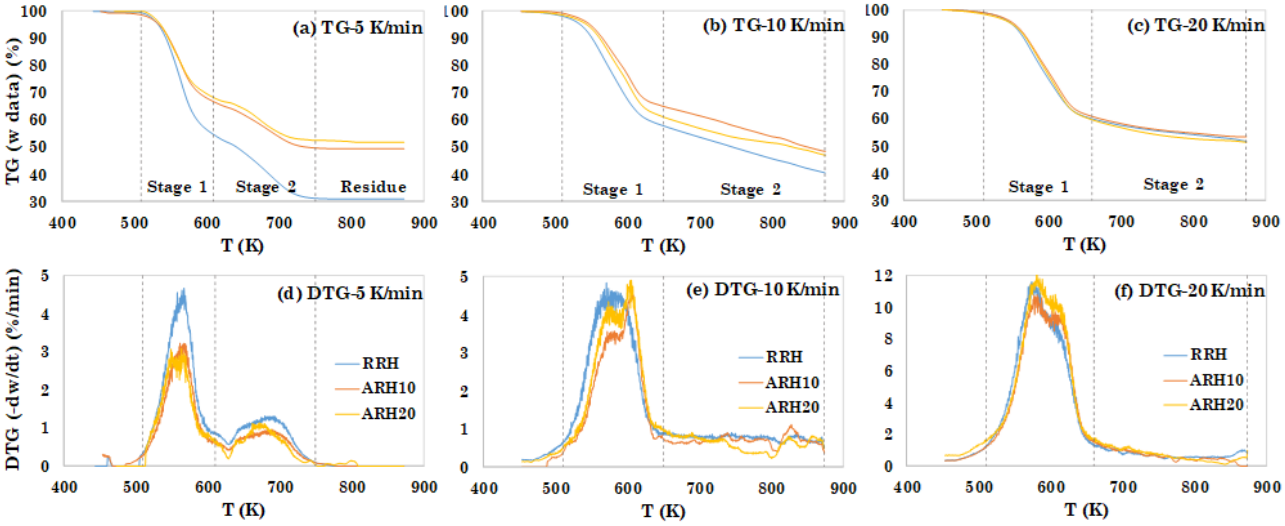

Figure 2. Generated TG (w) and DTG ($-dw/dt$) curves from experiment data.

of hemicellulose and cellulose at temperature between 530 and 650 K, and lignin decomposition at temperature between 650 and 1173 K. Refers to Yang [41], hemicellulose has a large number of compounds with C=O bonds that decompose in the temperature range of 473-588 K, while cellulose contains two strong −OH and C−O functional groups, which decompose in the temperature range of 588-673 K. Lignin decomposes over a wider temperature range because it has very strong bonds in aromatic ring structures (e.g., phenol and benzene). It is rich in $O-CH_3$, C−O−C, and C=C bonds, which require a wide temperature range to decompose completely. Furthermore, hemicellulose and lignin contribute to the amount of residue yielded; both leave solid residues despite being pyrolyzed at high temperatures.

3.3.1 Effect of Heating Rate

The thermogram curves in Figure 2(a-f) shows that the patterns of TG (w) and DTG ($-dw/dt$) curves can be different from each other depending on the heating rate. Increasing the heating rate shifts the TG curve towards higher temperatures. Besides, the higher the heating rate, the wider and higher the peaks of the DTG curve, shifting towards higher temperatures. The same trend was also reported by previous researchers [40,42,43]. This phenomenon assumably occurs because of the thermal lag during the biomass decomposition process due to the heat transfer and the kinetics of decomposition of rice husk pellets at different heating rates [44].

At low heating rates, there are two peaks in the DTG curve that are quite far apart from each other. The different profiles of the TG and DTG curves are observed at higher heating rates, where there are no longer two separate peaks, but there is one peak with a shoulder on the left or right of the DTG curve's peak. The shoulders and peaks formed on the DTG curve represent the decomposition of hemicellulose and cellulose. A gentle DTG curve at high temperatures representates a slower lignin decomposition step over a wide temperature range [40]. The DTG curve also indicates that the peak of mass loss rate (maximum decomposition rate) for non-catalytic and catalytic pyrolysis tends to increase and shift towards higher temperatures along with the increase in heating rate.

Based on Table 3 of non-catalytic pyrolysis (RRH), an increase in the heating rate tends to reduce the percentage of mass loss in Stage 1. Meanwhile, an increase in the heating rate in catalytic pyrolysis (ARH10 and ARH20) increases the percentage of mass loss in Stage 1. Furthermore, increasing the heating rate tends to reduce the percentage of mass loss in Stage 2 in both non-catalytic and catalytic pyrolysis. On the other hand, the residue tends to increase significantly along with the increase in the heating rate in non-catalytic pyrolysis (RRH). Higher conversions are obtained in pyrolysis with low heating rates. The same trend was reported by Quiroga [18] and Mishra & Mohanty [45] which states that at a higher heating rate, biomass does not decompose completely, thus producing more residue. In catalytic pyrolysis (ARH10 and ARH20), the percentage of residue produced tends not to change with the increasing of the heating rate. Based on the description, the effect of increasing the heating rate on the catalytic activity of ash is quite sensitive to both decompositions in Stage 1 and Stage 2. The ash can increase the

Table 3. Mass loss (%) for each stage and the residue (Data and 3-IPR model).

Non-catalytic	RRH-5		RRH-10		RRH-20	
	Data	3-IPR	Data	3-IPR	Data	3-IPR
Stage 1	43.6	43.4	41.3	38.6	39.5	38.5
Stage 2	25.7	22.3	18.3	19.3	8.8	8.1
Residue	30.7	34.3	40.3	42.1	51.7	53.4
Catalytic	ARH10-5		ARH10-10		ARH10-20	
	Data	3-IPR	Data	3-IPR	Data	3-IPR
Stage 1	31.9	31.7	34.0	34.1	38.5	38.4
Stage 2	18.8	19.3	17.6	17.6	8.1	8.1
Residue	49.3	49.0	48.4	48.4	53.3	53.6
Catalytic	ARH20-5		ARH20-10		ARH20-20	
	Data	3-IPR	Data	3-IPR	Data	3-IPR
Stage 1	30.3	31.9	38.1	37.8	39.6	39.5
Stage 2	18.2	17.9	14.9	14.6	9.3	8.8
Residue	51.6	50.2	47.0	47.6	51.1	51.7

percentage of mass loss in Stage 1, but tends to decrease that in Stage 2 with increasing heating rate. This phenomenon results in the insensitive decrease of residue percentage to the increase of heating rate in catalytic pyrolysis.

3.3.2 Effect of Ash Addition

Figure 2(a-f) show that at the same heating rate, the TG and DTG curves for non-catalytic pyrolysis (RRH) and catalytic pyrolysis (ARH10, ARH20) are identical. The similar result has been reported by Loy [40]. The increase in the ratio of ash addition shifts the TG and DTG curves sligthly towards higher temperatures because of the differences in heat transfer and pyrolysis kinetics as a result of the ash addition. The effect of increasing the ratio of ash addition is not quite visible at heating rate of 20 K/min, where the TG curve tends to coincide. However, the effect of ash addition is seen around the peak of the DTG curve at temperatures between 550-620 K, in accordance with the results of research by Milosalvjevic and Suuberg in Orfao [46] that pyrolysis kinetics changes at temperature of around 600 K. The DTG curve indicates that the peak of mass loss rate curve tends to decrease at low heating rates for catalytic pyrolysis or even slightly higher than in non-catalytic pyrolysis at high heating rates.

In Table 3 (column Data), the effect of increasing the ratio of ash addition to the mass loss in each stage and the percentage of residue is quite visible at low heating rates (5 and 10 K/min). The higher the ratio of ash addition the lower the mass loss percentage in Stage 1 and Stage 2, and the higher the residue. Meanwhile, at 20 K/min, the increase in the ratio of ash addition does not have a significant effect. In non-catalytic pyrolysis (RRH), the mass loss percentages in Stage 1 and Stage 2 range from 39.5% to 43.6% and from 8.8% to 25.7%, respectively, with residue of 30.7-51.7%. In catalytic pyrolysis (ARH10), the mass loss percentages in Stage 1 and Stage 2 ranges from 31.9% to 38.5% and from 8.1% to 18.8%, respectively, while residue of 48.4-53.3%. Meanwhile, in catalytic pyrolysis (ARH20), the mass loss percentages of Stage 1 and Stage 2 were 30.3-39.6% and 9.3-18.2%, respectively, with residue of 47.0-51.6%.

The addition of ash as a catalyst tends to reduce the mass loss percentages in Stage 1 and Stage 2 and increase the amount of residue therein. These findings are in accordance with those found by Loy [40] in the catalytic pyrolysis of rice husk with a mechanical mixing method. The increase in residue with the increasing the amount of ash catalyst is assumably due to the formation of coke on the surface of the catalyst as a result of the secondary tar cracking reactions [47,48]. At a heating rate of 20 K/min, the increase in the ratio of ash addition does not significantly affect the percentage of residue, assumably due to the tar cracking reaction that occurs and produces more gas. Furthermore, the effect of catalysis activity on hemicellulose, cellulose, and lignin decomposition needs to be further studied, given that there is a decrease in mass loss in Stage 1 (representing hemicellulose and cellulose decomposition) and Stage 2 (representing lignin decomposition) as a result of ash catalyst addition.

3.3.3 Controlling Regime

To determine the regime that controls the reaction, the parameters for calculating the *Py* number and *Bi* number in Equations (13-15) needs to be specified. The heat transfer from the heating surface to the biomass particles is mostly governed by the ratio of gas and solid turbulence in the reactor. Previous study had reported that the convective heat transfer coefficient for fixed-bed reactor with forced gas flow (similar in TGA) is in the range of 50-100 W/m^2.K [49]. Since the TGA equipment was used in this study, the average convective heat transfer coefficient (h) of 75 W/m^2.K was chosen. Whereas, the size of rice husk pellet used in this study was 3.21 mm (radius of pellet = 1.605 mm).

The addition of rice husk ash as catalyst may change the heat conductivity, heat capacity, and density of rice husk pellets. The heat conductivity of rice husk (λ_{RH}) and rice husk ash (λ_{ash}) as reported by previous studies were 5.0 W/m.K [3] and 0.4713 W/m.K [50], respectively. Meanwhile, the heat capacity of rice husk (C_{pRH}) and rice husk ash (C_{pash}) as a function of temperature were $C_{pRH} = 420 + 2.09T + 6.85\times10^{-4}T^2$ (J/kg.K) and $C_{pash} = 950 + 0.188T$ (J/kg.K), respectively [51]. Furthermore, the density of the pellet obtained from the measurement were 1,024 and 1,060 kg/m^3 for RRH and ARH10, respectively.

The reaction rate constant (k) was calculated using the Arrhenius equation with the kinetic parameters E_a and A obtained from previous study. Loy [3] conducted a pyrolysis of a mixture of rice husk powder and rice husk ash (with mass ratio of RH:ARH = 10:1) from 323 – 1173 K at a heating rate of 10-100 K/min with a N_2 flow rate of 100 mL/min. Determination of

the kinetic parameters in their study was carried out using the Friedman model-free method. The obtained average values of E_a and A for RRH pyrolysis were 190.8 kJ/mol and 2.27×10^{14} (1/s), respectively, and for ARH10 pyrolysis were 152.6 kJ/mol and 5.72×10^{11} (1/s), respectively.

Furthermore, the Py^{I}, Py^{II}, and Bi numbers were calculated at pyrolysis temperature range between 450-750 K with an interval of 50 K. Then, plotting the results into reaction-transport map [33] will obtain the information on the controlling regime as shown in Figure 3. It can be seen that the mechanisms of non-catalytic pyrolysis (RRH) and catalytic pyrolysis (ARH10) of rice husk pellets are dominated in the isothermal kinetically-limited region, especially at low temperatures. An increase in the reaction temperature will increase the reaction rate thereby shifting the reaction towards convection-limited region. It is quite difficult to accommodate shifts in the limiting region that occur at high temperatures in the kinetics modeling of pyrolysis reactions. Furthermore, the calculation of the kinetics model is only based on the mechanism which is limited by isothermal kinetics.

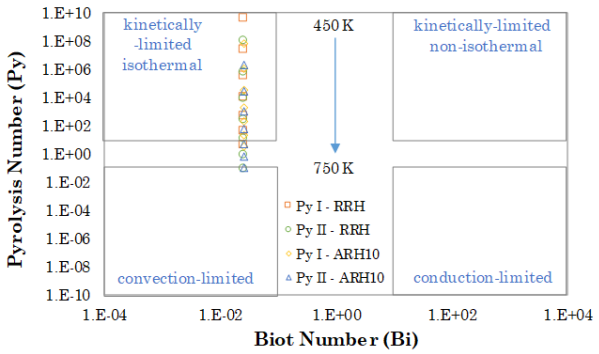

Figure 3. Reaction-transport map for rice husk pellet pyrolysis.

3.4 Kinetic Parameters of the 3-IPR Model

Figure 4(a-i) show the profiles of the DTG ($-dw/dt$) curve generated by the 3-IPR model (black solid line) and those of decomposition of hemicellulose, cellulose, and lignin (gray dashed line) at various heating rates and ash addition ratios. The 3-IPR model accurately represents the experimental data (blue line). The model accuracy can also be seen in the percentages of mass loss in each stage and the percentages of residue in Table 3 (in 3-IPR column) that are not much different from those in the experimental data. In more detail, the DTG curve for each component at various heating rates and ash addition ratios is presented in Figure 5(a-i).

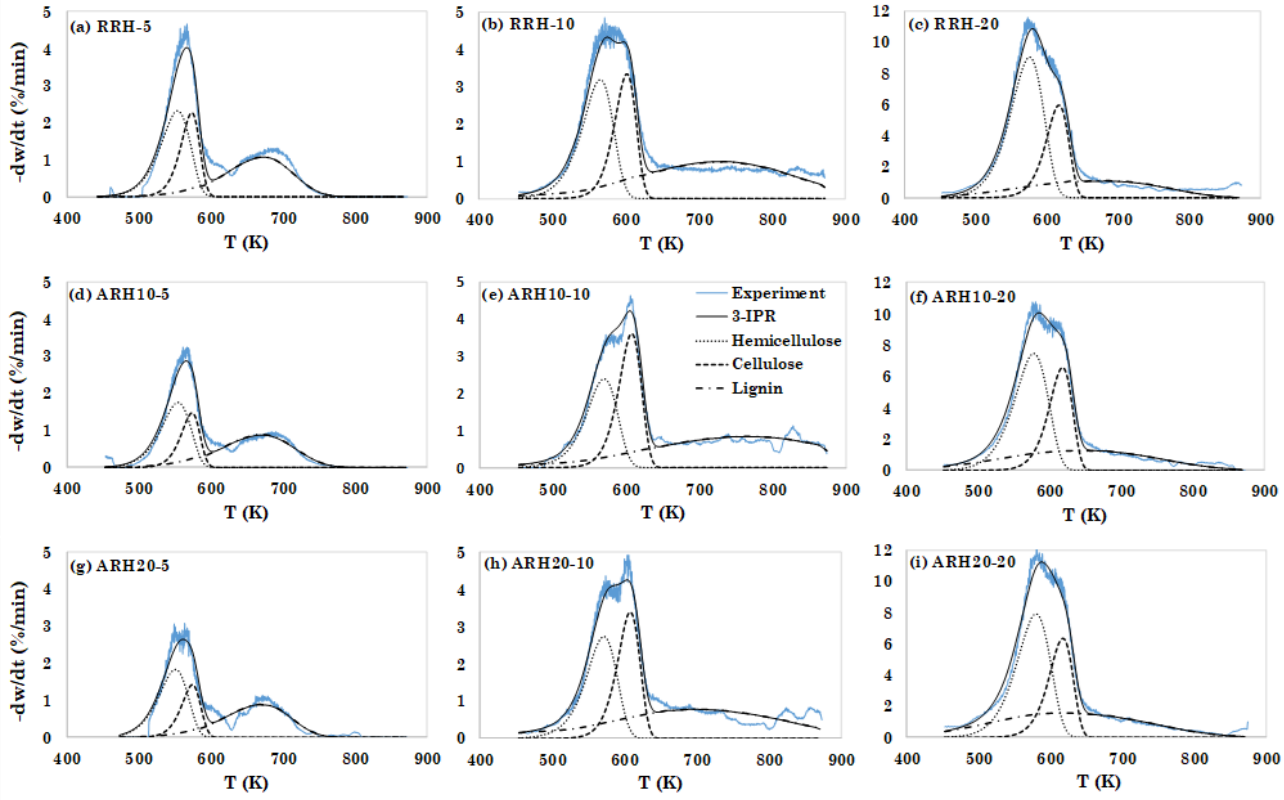

Figure 4. Generated DTG curves from the experiment data and the 3-IPR model.

The mass loss rate curves for each component as presented in Figure 5(a-i) are identical; each has a main peak, as also reported by previous study [20]. In thermogravimetric analysis, the temperature characteristics of the DTG curve, namely T-onset, T-offset, and T-max, depend on the heating rate. Many studies state that the use of low heating rates (≤20 K/min) is prioritized to determine these temperature characteristics [20]. T-onset is the temperature at which a pyrolysis stage begins, and T-offset is the temperature at which a pyrolysis stage is completed. T-onset and T-offset are obtained from the tangential intersection of the DTG curve at the bottom of the curve. Meanwhile, T-max is the temperature where the peak of the DTG curve appears and is obtained from the tangential intersection of the DTG curve at

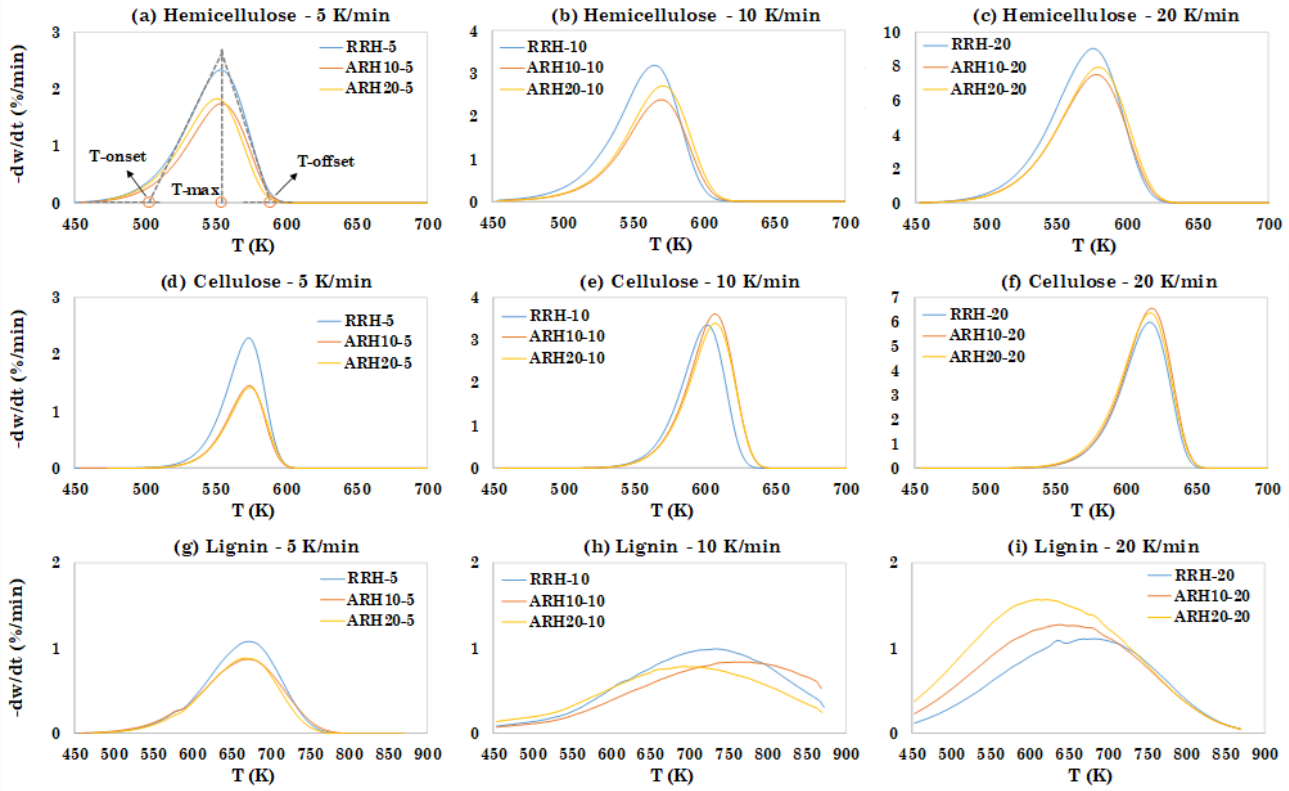

Figure 5. Effect of heating rate and ash addition ratio on component decomposition.

Table 4. Thermal characteristics of rice husk component decomposition (3-IPR).

Non-catalytic	RRH-5			RRH-10			RRH-20		
	Hemi.	Cell.	Lign.	Hemi.	Cell.	Lign.	Hemi.	Cell.	Lign.
T-onset (K)	501	538	565	511	564	505	517	576	453
T-offset (K)	589	596	753	600	628	893	615	644	844
−dw/dt max	2.332	2.278	1.069	3.197	3.349	0.990	9.046	5.971	1.104
T-max (K)	557	575	675	567	602	734	578	619	684
Catalytic	ARH10-5			ARH10-10			ARH10-20		
	Hemi.	Cell.	Lign.	Hemi.	Cell.	Lign.	Hemi.	Cell.	Lign.
T-onset (K)	500	538	542	516	567	495	517	576	431
T-offset (K)	589	596	761	606	634	1032	619	646	844
−dw/dt max	1.744	1.454	0.871	2.381	3.601	0.837	7.498	6.546	1.269
T-max (K)	556	576	677	571	609	761	580	620	645
Catalytic	ARH20-5			ARH20-10			ARH20-20		
	Hemi.	Cell.	Lign.	Hemi.	Cell.	Lign.	Hemi.	Cell.	Lign.
T-onset (K)	498	539	559	516	568	469	521	573	417
T-offset (K)	587	598	750	609	635	935	620	645	840
−dw/dt max	1.821	1.413	0.877	2.719	3.382	0.777	7.913	6.345	1.560
T-max (K)	552	575	674	573	609	704	583	619	622

the top of the curve. For example, the DTG curve characterization for hemicellulose at a heating rate of 5 K/min is shown in Figure 5(a). Moreover, the results of the DTG curve characterization are presented in Table 4.

3.4.1 Effect of heating rate on component decomposition

Figure 4(a,d,g) show that at a low heating rate (5 K/min), the peaks formed have narrower characteristics; hemicellulose and cellulose contribute to the formation of the peaks. The narrower peak for rice husk pyrolysis at low heating rate (5 K/min) with the contribution of hemicellulose and cellulose decomposition was also observed by Ferreiro [15]. Meanwhile, at higher heating rates (10 and 20 K/min), there were shoulders and peaks on the DTG curves; hemicellulose and cellulose alternated with each other to contribute to the formation of peaks and shoulders in the DTG curves. At a heating rate of 10 K/min (Figure 4(b,e,h)), cellulose decomposition contributes more dominantly to the formation of the peaks of the DTG curves, while hemicellulose decomposition does so to the formation of the shoulders at lower temperatures. A significant difference occurs at a heating rate of 20 K/min (Figure 4(c,f,i)), in which the contribution of hemicellulose decomposition to the peak is more dominant, and the decomposition of cellulose contributes to the formation of the shoulders at higher temperatures. At a high heating rate, the contribution of lignin decomposition at a higher rate is started to appear since the early stages of pyrolysis. Therefore, at a high heating rate, the addition of ash increases lignin mass loss rates starting at low temperatures.

Heating rate has a significant effect on the maximum mass loss rate ($-\mathrm{d}w/\mathrm{d}t$ max) for hemicellulose, cellulose, and lignin (see Table 4 and Figure 5(a-i)). The increase in heating rate increases the maximum mass loss rate, both for non-catalytic pyrolysis and catalytic pyrolysis. The same trend was also reported by previous studies [3,15]. Likewise, T-max tends to shift towards higher temperatures as the heating rate increases. Increasing the heating rate from 5 K/min to 10 K/min will increase the T-max to about 10-20 K for hemicellulose, 25-35 K for cellulose, and 30-85 K for lignin decomposition. This finding is comparable to previous study in the pyrolysis of switchgrass [21], the increase in the heating rate from 25 K/min to 100 K/min provides the increase of the T-max around 30 K for all components.

3.4.2 Effect of ash addition on component decomposition

The addition of ash tends to reduce the maximum mass loss rate for all components at low heating rates (see Table 4 and Figure 5(a,d,g)). However, at higher heating rates, the maximum mass loss rates of cellulose and lignin in Figure 5(e,f,h,i) increase as a result of the addition of ash. In Table 4, the range of hemicellulose decomposition temperatures in the non-catalytic pyrolysis (and the catalytic pyrolysis) is shown between 501-615 K (498-620 K) with T-max of 557-578 K (552-583 K). Meanwhile, the cellulose decomposition temperatures range between 538-644 K (538-646 K) with T-max of 575-619 K (575-620 K). Furthermore, lignin decomposition occurs over a wider temperature range of 453-893 K (417-935 K) with T-max of 675-734 K (622-761 K). These ranges of decomposition temperatures and maximum decomposition temperatures are in accordance with previous studies [17,19,20,41]. The addition of ash tends to widen the components' decomposition temperature and maximum decomposition temperature ranges.

Figure 5(a-f) say that T-max(s) of hemicellulose and cellulose tend to be higher in catalytic pyrolysis, in contrast to lignin decomposition (Figure 5(g-i)) whose maximum decomposition temperature tends to be lower, in accordance to the results of [21]. These data indicate that lignin decomposition occurs more easily [52] in catalytic pyrolysis than in the non-catalytic. The difference in the decomposition temperature range of each component is caused by differences in the chemical structures. Hemicellulose consists of various saccharides (xylose, mannose, glucose, galactose, *etc.*), with random, amorphous, and many-branched structures that are very easily decomposed to produce volatiles at low temperatures. Cellulose consists of long and straight glucose polymers without branches and is well structured and very strong, thus having a higher thermal stability than hemicellulose. Meanwhile, lignin is full of aromatic rings with various kinds of branches. Chemical bonds in lignin are numerous, causing lignin decomposition to occur over a wide temperature range [41].

The description indicates that the catalytic effect of the ash on the mass loss rate appears at high heating rates with greater ash addition ratios only. High mass loss rates at high heating rates are assumably related to increased catalytic activity at higher heating rates [21]. Meanwhile, the use of a high heating rate and

Table 5. Kinetics parameters of the 3-IPR model.

Parameters	Non-catalytic			Catalytic				
	RRH-5	RRH-10	RRH-20	ARH10-5	ARH10-10	ARH10-20	ARH20-5	ARH20-10	ARH20-20
Ea_{hc}	123.12	122.25	122.30	123.21	123.42	121.53	122.42	123.81	123.24
Ea_{cel}	210.00	205.00	210.06	210.00	201.37	206.09	210.00	199.94	201.24
Ea_{lig}	77.16	35.79	40.00	68.98	31.90	34.59	76.78	29.01	32.50
A_{hc}	1.00×10^{11}	1.00×10^{11}	1.01×10^{11}	1.00×10^{11}	9.94×10^{10}	7.60×10^{10}	1.00×10^{11}	1.00×10^{11}	1.00×10^{11}
A_{cel}	5.06×10^{18}	4.42×10^{17}	7.58×10^{17}	4.94×10^{18}	1.38×10^{17}	3.16×10^{17}	4.60×10^{18}	1.00×10^{17}	1.27×10^{17}
A_{lig}	1.00×10^{05}	3.00×10^{01}	2.35×10^{02}	2.15×10^{04}	1.00×10^{01}	9.78×10^{01}	1.00×10^{05}	1.00×10^{01}	7.10×10^{01}
c_{hc}	0.250	0.200	0.219	0.187	0.146	0.184	0.193	0.166	0.183
c_{cel}	0.157	0.132	0.116	0.100	0.150	0.130	0.100	0.143	0.123
c_{lig}	0.250	0.262	0.132	0.224	0.267	0.152	0.205	0.228	0.178
n	1	1	1	1	1	1	1	1	1
Fit(%)	*3.140*	*3.008*	*0.859*	*3.423*	*2.205*	*0.723*	*4.782*	*2.709*	*0.598*
R^2	*0.97*	*0.97*	*0.99*	*0.97*	*0.99*	*0.99*	*0.95*	*0.97*	*0.99*

ash addition ratios actually reduces the mass loss rate of hemicellulose, although not too significant. This fact indicates that the catalytic activity of the ash appears at high temperatures when the decomposition of cellulose and lignin is more dominant.

Furthermore, the kinetics parameter values of non-catalytic pyrolysis (RRH) and catalytic pyrolysis (ARH10 and ARH20) of the 3-IPR model for each component are presented in Table 5. It can be seen that the values of the coefficient of determination (R^2) for all samples are in the range of 0.95-0.99. Meanwhile, the fitness (fit(%)) values for all samples are below 5%. These data indicate that the 3-IPR kinetics model can describe the non-catalytic and catalytic pyrolysis reactions of rice husk pellets well.

The apparent activation energy (E_a) value in Table 5 for the decomposition of hemicellulose tends to be constant at the various heating rates. Meanwhile, the E_a values for the decomposition of cellulose and lignin tend to decrease by increasing heating rate. Based on these data, the use of a higher heating rate is more beneficial in terms of decreasing the E_a. This finding is also corroborated by the average E_a value of all components at various heating rates as shown in Figure 6(a). It appears that the catalytic effect of husk ash on decreasing the value of E_a is found to be more significant at a higher heating rate.

As in Table 5, the addition of ash as a catalyst has no effect on the E_a of hemicellulose de-

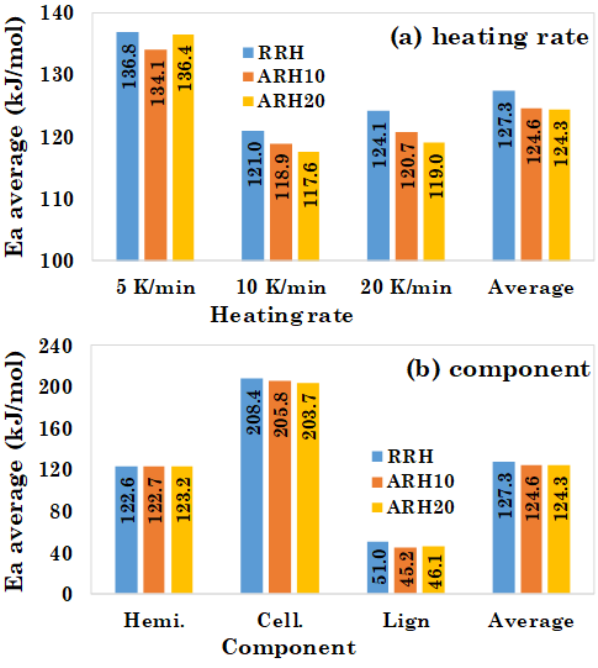

Figure 6. The average E_a of 3-IPR model: (a) for each heating rate; (b) for each component.

composition. It only has a minor effect on the E_a values of cellulose and lignin decomposition by decreasing them slightly. The average E_a value of each component for the entire range of heating rate values as shown in Figure 6(b) confirm the finding. It can be seen that the catalytic pyrolysis has no effect on the E_a value of hemicellulose, but slightly decreases the E_a values of cellulose and lignin.

The average E_a values of hemicellulose, cellulose, and lignin for the entire range of heating rate in the non-catalytic pyrolysis (RRH pyrolysis) are 122.6, 208.4, and 51.0 kJ/mol, respectively. For the comparison, Ferreiro [15] studied the non-catalytic pyrolysis of rice husk powder (size < 1 mm) at the heating rate of 5-15 K/min. They found that the E_a values calculated using first order 3-IPR kinetics model for hemicellulose, cellulose, and lignin were 107.3, 163.8, and 37.2 kJ/mol, respectively. The same kinetic model was also used by Garba [16] in the non-catalytic pyrolysis of rice husk powder (size < 150 μm) at the heating rate of 10 K/min. In their study, the E_a values of hemicellulose, cellulose, and lignin were 90.0, 187.0, and 29.0 kJ/mol, respectively. The higher E_a values yielded from our study may be due to the contribution of external and/or internal heat transfer resistance in pyrolysis reaction of larger particles.

For the catalytic pyrolysis of rice husk pellets (e.g ARH20), the average E_a values for hemicellulose, cellulose, and lignin are found to be 123.2, 203.7, and 46.1 kJ/mol, respectively. As mentioned before, the addition of husk ash has only a minor effect in decreasing the average E_a values of cellulose and lignin decomposition. The use of mineral-based catalysts in biomass pyrolysis has reported by Mohamed [21]. By using the 3-IPR kinetics model, this study proofed that the addition of 30% by weight of different catalyst (*i.e.* K_3PO_4, natural zeolite, and bentonite) into switchgrass powder can significantly decrease the E_a values of all components. Pyrolysis at 25 K/min decrease the E_a value for hemicellulose from 105.0 kJ/mol to 90.2-98.1 kJ/mol, cellulose from 241.0 kJ/mol to 164.0-194.0 kJ/mol, and lignin from 47.3 kJ/mol to 37.8-38.4 kJ/mol. In addition, the calculated reaction order were found to be close to 1 for all components.

As shown in Figure 6, the overall average E_a values reduces from 127.3 kJ/mol (for RRH pyrolysis) to 124.3 kJ/mol (in ARH20 pyrolysis). As a comparison, the catalytic pyrolysis of bagasse conducted by Quiroga [18] using the catalyst Rh-Pt/CeO_2-SiO_2 showed that the overall E_a calculated by using the 3-IPR model reduced from 120.9 kJ/mol to 107.0 kJ/mol. Fu [52] conducted a catalytic pyrolysis of rice husk with the addition of the catalyst solid KOH. The E_a value obtained by the model-free method reduced from 123.8 kJ/mol to 75.9 kJ/mol. Loy [3] also conducted research on the catalytic pyrolysis of rice husk with husk ash as a catalyst. The decreased average E_a value from 190 kJ/mol to 153 kJ/mol was found using the model-free method. In our previous report [10], the kinetics of catalytic pyrolysis of rice husk pellet with the addition of husk ash was studied by using the model-free method. The calculated average E_a values by Friedman method at rapid mass loss stage reduced from 191.0 kJ/mol to 112.3 kJ/mol. Comparation of studies appears that the use of different kinetic models provides a significant difference in the calculated E_a values.

The activity of the husk ash for reducing E_a values in this study was much lower than other mineral-based catalysts. This was reasonable because the rice husk ash used in our study was not subjected to any treatment. The lower reduction of E_a in this study is also assumably due to the higher temperature of the catalyst preparation of 1073 K. As mentioned in the introduction, whereas, the optimum temperature for the ash catalyst preparation through burning rice husk is 773 K [3,12]. The use of higher temperatures in the ash catalyst preparation in this preliminary study was intended to approach the gasification process temperature, where the ash produced could be directly used as a low-cost catalyst.

Nevertheless, the improvement of the catalytic activities of husk ash needs to be addressed for further studies. The proper temperature of rice husk combustion in an controllable manner for ash production needs to be studied in order to achieve the best catalytic activities of husk ash. Besides, the impregnation of metal-based catalysts on husk ash will absolutely increase its activities, but this process offers the high production cost. In terms of in-situ catalytic thermochemical process as proposed in this study, the difficulties to separate the catalyst from the pyrolysis or gasification solid product need to be considered, so a low-cost and disposable catalyst is needed. To address these criteria, husk ash which is generated from gasification process is possibly to be used first as an adsorbent of metallic pollutants in wastewater prior to catalyst. As reported in previous studies [54-56], rice husk ash has a good ability in metallic pollutants adsorption.

In the other hand, Table 5 shows that the pre-exponential factor (A) for hemicellulose decomposition is relatively constant at various heating rates and ash addition ratios, in the range of 7.60×10^{10}–1.00×10^{11} (1/min). Meanwhile, the A values for the decomposition of cellulose and lignin vary between the different heating rates. However, at the same heating rate, the addition of ash does not have a major effect on the A value. The range of A value for cellulose decomposition (1.00×10^{17}–5.06×10^{18} (1/min)) is narrower than it for lignin decomposition (1.00×10^{01}–1.00×10^{05} (1/min)). As shown in Table 5, the addition of husk ash catalyst tends to lower the A values. It seems that there is a compensation effect of the E_a value and the A value, that is, the lower the value of E_a, the lower the value of A. The lower of A values as an effect of catalyst addition and the compensation effect were also observed in previous studies [18,21]. Furthermore, the partial contribution (c_i) of each component varies at different heating rates and ratios of ash addition. In the non-catalytic pyrolysis (and the catalytic pyrolysis), the range of c_i values for hemicellulose, cellulose, and lignin are 0.20-0.25 (0.15-0.19), 0.12-0.16 (0.10-0.15), and 0.13-0.26 (0.15-0.27), respectively.

Apart from the influence of the type of catalyst, the use of different kinetic models can also produce a significant difference of E_a values. Regardless the use of different kinetic models, the rice husk ash added to rice husk pellets can actually reduce the apparent activation energy of pyrolysis, which in turn increase the reaction rate constant. Based on the average A value of each the heating rate and the E_a value of each component in Table 5, the reaction rate constant is then calculated using the Arrhenius equation. The results of the reaction rate constant values for each component at various temperatures are presented in Table 6. An increase in temperature can increase the reaction rate constant significantly, which in turn increase the reaction rate. At low temperatures, the reaction rate of lignin decomposition is higher than those of hemicellulose and cellulose decomposition. However, starting at 550 K, the decomposition reaction rates of hemicellulose and cellulose are higher than that of lignin. In this study, the addition of the ash tended to reduce insignificantly the hemicellulose decomposition rate. Meanwhile, the increase in the lignin decomposition rate was more significant than that in cellulose decomposition, indicating that the catalytic activity of the ash appeared at high temperatures.

4. Conclusions

The proposed different method of husk ash catalyst addition in the in-situ catalytic pyrolysis of rice husk pellets has been investigated on the thermal characteristics and pyrolysis kinetics of the biomass components. This preliminary study found that pyrolysis of rice husk pellets is divided into two stages, namely Stage 1 at a temperature range of 510-650 K representing hemicellulose and cellulose decomposition, and Stage 2 at temperatures above 650 K representing lignin decomposition. The addition of ash as a catalyst in the catalytic pyrolysis of rice husk pellets tends to reduce the mass loss both in Stage 1 and Stage 2 and increase the solid residue. The addition of the ash also tends to widen the decomposition temperature range and the maximum decomposition temperature of each component.

The addition of the ash tends to decrease the maximum mass loss rate of the three components at low heating rates. However, at higher heating rates, there is an increase in the maximum mass loss rates of cellulose and lignin. In other words, the catalytic activity of the ash appears at high heating rates and high temperatures where the decompositions of cellulose and lignin are more dominant.

Based on the values of coefficient of determination (R^2) and fitness (fit(%)), it can be con-

Table 6. Component reaction rate constant (1/min).

Temp. (K)	Hemicellulose			Cellulose			Lignin		
	RRH	ARH10	ARH20	RRH	ARH10	ARH20	RRH	ARH10	ARH20
450	0.0006	0.0006	0.0005	0.0000	0.0000	0.0000	0.0014	0.0057	0.0100
500	0.0153	0.0149	0.0134	0.0002	0.0003	0.0004	0.0042	0.0150	0.0235
550	0.2236	0.2177	0.1975	0.0225	0.0276	0.0364	0.0105	0.0354	0.0477
600	2.0863	2.0327	1.8612	1.0222	1.2207	1.5448	0.0237	0.0773	0.0881
650	13.804	13.465	12.420	25.853	30.182	36.996	0.0502	0.1601	0.1521
700	69.726	68.090	63.198	412.350	472.874	565.119	0.1012	0.3161	0.2523
750	283.805	277.433	258.881	4547.57	5140.59	6019.10	0.1953	0.5945	0.4079

cluded that the 3-IPR kinetics model describes the pyrolysis reaction of rice husk pellets well. The addition of the ash tends to have no effect on the activation energy of hemicellulose decomposition but decreases the activation energy of cellulose and lignin decompositions. Meanwhile, at the same heating rate, the addition of husk ash catalyst to rice husk pellets does not significantly affect the pre-exponential factor. In addition, the ash tends to decrease the hemicellulose decomposition rate and increase the cellulose and lignin decomposition rates.

The heating rates and the ash addition ratios both affect the activation energy of each component, but the values were not always lower in catalytic pyrolysis. However, the average activation energy decreases with increasing heating rate and ash addition. Nonetheless, there is only a relatively minor change in the average activation energy as the husk ash catalyst was added. The improvement of this untreated husk ash catalyst need to be addressed to obtain the low-cost, disposable, and more active catalyst.

Acknowledgments

The authors gratefully thank the Directorate General of Higher Education, Ministry of Research Technology and Higher Education, the Republic of Indonesia for the support and funding.

References

[1] Wang, S-W, Li, D-X., Ruan, W-B., Jin, C-L., Farahani, M.R. (2018). A techno-economic review of biomass gasification for production of chemicals. *Energy Sources, Part B: Economics, Planning, and Policy*, 13(8), 351-356. DOI: 10.1016/j.egypro.2017.03.1111.

[2] Muneer, B., Zeeshan, M., Qaisar, S., Razzaq, M., Iftikhar, H. (2019). Influence of in-situ and ex-situ HZSM-5 catalyst on co-pyrolysis of corn stalk and polystyrene with a focus on liquid yield and quality. *Journal of Cleaner Production*, 237, 117762. DOI: 10.1016/j.jclepro.2019.117762.

[3] Loy, A.C.M., Gan, D.K.W., Yusup, S., Chin, B.L.F., Lam, M.K., Shahbaz, M., Unrean, P., Acda, M.N., Rianawati, E. (2018). Thermogravimetric kinetic modeling of in-situ catalytic pyrolytic conversion of rice husk to bioenergy using rice hull ash catalyst. *Bioresource Technology*, 261, 213-222. DOI: 10.1016/j.biortech.2018.04.020.

[4] Chen, Z., Zhang, L. (2015). Catalyst and process parameters for the gasification of rice husk with pure CO_2 to produce CO. *Fuel Processing Technology*, 133, 227-231. DOI: 10.1016/j.fuproc.2015.01.027.

[5] Prabahar, R.S.S., Nagaraj, H., Jeyasubramanian, K. (2019). Enhanced recovery of H2 gas from rice husk and its char enabled with nano catalytic pyrolysis/gasification. *Microchemical Journal*, 146, 922-930. DOI: 10.1016/j.microc.2019.02.024.

[6] Hidayat, A., Adnan, M.A., Sahid., A.C.M. (2020). Catalytic pyrolysis of Palm Empty Fruit Bunch over activated natural dolomite catalyst: Product distribution and product analysis. *Material Science Forum*, 991, 111-116. DOI: 10.4028/www.scientific.net/MSF.991.111.

[7] Yuan, R., Yu, S., Shen, Y. (2019). Pyrolysis and combustion kinetics of lignocellulosic biomass pellets with calcium-rich wastes from agroforestry residues. *Waste Management*, 87, 86-96. DOI: 10.1016/j.wasman.2019.02.009.

[8] Yuan, R., Shen, Y. (2019). Catalytic pyrolysis of biomass-plastic wastes in the presence of MgO and $MgCO_3$ for hydrocarbon-rich oils production. *Bioresources Technology*, 293, 122076. DOI: 10.1016/j.biortech.2019.122076.

[9] Pradana, Y.S., Daniyanto, Hartono, M., Prasakti, L., Budiman, A. (2019). Effect oc calcium and magnesium catalyst on pyrolysis kinetic of Indonesian sugarcane bagasse for biofuel production. *Energy Procedia*, 158, 431-439. DOI: 10.1016/j.egypro.2019.01.128.

[10] Wibowo, W. A., Cahyono, R. B., Rochmadi, R., Budiman, A. (2022). Thermogravimetric Analysis and Kinetic Study on Catalytic Pyrolysis of Rice Husk Pellet using Its Ash as a Low-cost In-situ Catalyst. *International Journal of Renewable Energy Development*, 11(1), 207-219. DOI: 10.14710/ijred.2022.41887

[11] Rong, C., Li, B., Liu, W., Zhao, N. (2018). The effect of oyster shell powder & rice husk ash on the pyrolysis of rice husk for bio-oil. *Energy Sources Part A: Recovery, Utilization, and Environmental Effects*, 40(11), 1291-1304. DOI: 10.1080/15567036.2018.1469690.

[12] Deshmukh, P., Bhatt, J., Peshwe, D., Pathak, S. (2012). Determination of Silica Activity Index and XRD, SEM and EDS Studies of Amorphous SiO_2 Extracted from Rice Husk Ash. *Transactions of the Indian Institute of Metals*, 65(1), 63-70. DOI: 10.1007/s12666-011-0071-z.

[13] Carrier, M., Auret, L., Bridgwater, A., Knoetze, J.H. (2016). Using Apparent Activation Energy as a Reactivity Criterion for Biomass Pyrolysis. *Energy Fuels*, 30, 7834 -7841. DOI: 10.1021/acs.energyfuels.6b00794.

[14] Santos, K.G., Lira, T. S., Gianesella, M., Lobato, F.S., Murata, V.V., Barrozo, M.A.S. (2012). Bagasse Pyrolysis: A Comparative Study of Kinetic Models. *Chemical Engineering Communications*, 199(1), 109-121. DOI: 10.1080/00986445.2011.575906.

[15] Ferreiro, A.I.M. (2015). Pyrolysis of Pine Bark, Wheat Straw and Rice Husk: Thermogravimetric Analysis and Kinetic Study. *Thesis report*. Mechanical Engineering – Tecnico Lisboa.

[16] Garba, M.U., Charise, S.G., Bilyaminu, I., Alhassan, M., Musa, U., Isah, A.G. (2016). Kinetic Modeling of Rice Husk Components Pyrolysis Based on Independent Parallel Reactions. *Nigeria Journal of Engineering and Applied Sciences*, 3(1), 35-42. http://repository.futminna.edu.ng:8080/jspui/handle/123456789/9211.

[17] Chen, W.H., Eng, C.F., Lin, Y.Y., Lin, Y.Y., Bach, Q.V. (2020). Independent parallel pyrolysis kinetics of cellulose, hemicelluloses and lignin at various heating rates analyzed by evolutionary computation. *Energy Conversion and Management*, 221, 113165. DOI: 10.1016/j.enconman.2020.113165

[18] Quiroga, E., Molto, J., Conesa, J.A., Valero, M.F., Cobo, M. (2020). Kinetics of the catalytic thermal degradation of Sugarcane residual biomass over Rh-Pt/CeO_2-SiO_2 for syngas production. *Catalysts*, 10, 508. DOI: 10.3390/catal10050508.

[19] Park, W.C., Atreya, A., Baum, H.R. (2010). Experimental and theoretical investigation of heat and mass transfer processes during wood pyrolysis. *Combustion and Flame*, 157, 481-494. DOI: 10.1016/j.combustflame.2009.10.006.

[20] Collard, F.X., Blin, J. (2014). A review on pyrolysis of biomass constituents: Mechanisms and composition of the products obtained from the conversion of cellulose, hemicelluloses and lignin. *Renewable and Sustainable Energy Reviews*, 38, 594-608. DOI: 10.1016/j.rser.2014.06.013.

[21] Mohamed, B.A., Ellis, N., Kim, C.S., Bi, X. (2020). Synergistic Effects of Catalyst Mixtures on Biomass Catalytic Pyrolysis. *Frontiers in Bioengineering and Biotechnology*, 8, 615134. DOI: 10.3389/fbioe.2020.615134.

[22] Shirazi, Y., Viamajala, S., Varanasi, S. (2020). In situ and Ex situ Catalytic Pyrolysis of Microalgae and Integration With Pyrolytic Fractionation. *Frontiers in Chemistry*, 8, 786. DOI: 10.3389/fchem.2020.00786.

[23] Lu, Q., Zhang, T., Deng, X., He, R., Yuan, S., Li, J., Xie, X., Li, W., Liu, Z., Zhang, X. (2020). Enhancement of gas and aromatics by in-situ catalytic pyrolysis of biomass in the presence of silica gel. *Biomass and Bioenergy*, 138, 105567. DOI: 10.1016/j.biombioe.2020.105567.

[24] Balasundram, V., Ibrahim, N., Kasmani, R.M., Abd. Hamid, M.K., Isha, R., Hasbullah, H., Ali, R.R. (2017). Thermogravimetric catalytic pyrolysis and kinetic studies of coconut copra and rice husk for possible maximum production of pyrolysis oil. *Journal of Cleaner Production*, 167, 218-228. DOI: 10.1016/j.jclepro.2017.08.173.

[25] Zabeti, M., Nguyen, T.S., Lefferts, L., Heeres, H.J., Seshan, K. (2012). In situ catalytic pyrolysis of lignocellulose using alkali-modified amorphous silica alumina. *Bioresource Technology*, 118, 374-381. DOI: 10.1016/j.biortech.2012.05.034.

[26] Jeon, M.J., Kim, S.S., Jeon, J.K., Park, S.H., Kim, J.M., Sohn, J.M., Lee, S.H., Park, Y.K. (2012). Catalytic pyrolysis of waste rice husk over mesoporous materials. *Nanoscale Research Letters*, 7(18), 1-5. http://www.nanoscalereslett. com/ content/7/1/18.

[27] Diez, D., Uruena, A., Pinero, R., Barrio, A., Tamminen, T. (2020). Determination of Hemicellulose, Cellulose, and Lignin Content in Different Types of Biomasses by Thermogravimetric Analysis and Pseudocomponent Kinetic Model (TGA-PKM Method). *Processes*, 8, 1048. DOI: 10.3390/pr8091048.

[28] Storn, R., Price, K. (1997). Differential Evolution – A Simple and Efficient Heuristic for Global Optimization over Continuous Spaces. *Journal of Global Optimization*, 11, 341–359. DOI: 10.1023/a:1008202821328

[29] Sheth, P.N., Babu, B.V. (2009). Differential Evolution Approach for Obtaining Kinetic Parameters in Nonisothermal Pyrolysis of Biomass. *Material and Manufacturing Processes*, 24, 47-52. DOI: 10.1080/10426910802540661.

[30] Dragoi, E.N., Curteanu, S. (2016). The use of differential evolution algorithm for solving chemical engineering problems. *Reviews in Chemical Engineering*, 32(2), 149-180. DOI: 10.1515/revce-2015-0042.

[31] Ahmad, M.F., Isa, N.A.M., Lim, W.H., Ang, K.M. (2022). Differential evolution: A recent review based on state-of-the-art works. *Alexandria Engineering Journal*, 61, 3831-3872. DOI: 10.1016/j.aej.2021.09.013.

[32] Wang, M. (2014). Optimization Rastrigin Function by Differential Evolution algorithm. Version 1.0.0.0. (https://www.mathworks.com/matlabcentral/fileexchange/46818-optimization-rastrigin-function-by-differential-evolution-algorithm), MATLAB Central File Exchange. Retrieved March 05, 2021.

[33] Paulsen, A.D., Mettler, M.S., Dauenhauer, P.J. (2013). The role of sample dimension and temperature in cellulose pyrolysis. *Energy Fuels*, 27(4), 2126–2134. DOI: 10.1021/ef302117j

[34] Rasool, T., Srivastava, V.C., Khan, M.N.S. (2018). Kinetic and thermodynamic analysis of thermal decomposition of Deodar (Cedrus Deodara) saw dust and rice husk as potential feedstock for pyrolysis. *International Journal of Chemical Reactor Engineering*, 17(1), 20170184. DOI: 10.1515/ijcre-2017-0184.

[35] Abaide, E.R., Tres, M.V., Zabot, G.L., Mazutti, M.A. (2019). Reasons for processing of rice coproducts: Reality and expectations. *Biomass and Bioenergy*, 120, 240-256. DOI: 10.1016/j.biombioe.2018.11.032.

[36] Jiang, L., Hu, S., Wang, Y., Su, S., Sun, L., Xu, B., He, L., Xiang, J. (2015). Catalytic effects of inherent alkali and alkaline earth metallic species on steam gasification of biomass. *International Journal of Hydrogen Energy*, 40, 15460-15469. DOI: 10.1016/j.ijhydene.2015.08.111.

[37] Wang, Z., Xiong, Y. (2020). Simultaneous improvement in qualities of bio-oil and syngas from catalytic pyrolysis of rice husk by demineralization. *Energy Sources, Part A: Recovery, Utilization, and Environmental Effects*, 42, 1-14. DOI: 10.1080/15567036.2020.1824038.

[38] Pradana Y.S., Hidayat, A., Prasetya, A., Budiman, A. (2018). Application of coconut-shell activated carbon as heterogeneous solid catalyst for biodiesel synthesis. *Defect and Diffusion Forum*, 382, 280-285. DOI: 10.4028/www.scientific.net/DDF.382.280.

[39] Shen, Y., Zhao, P., Shao, Q., Ma, D., Takahashi, F., Yoshikawa, K. (2014). In-situ catalytic conversion of tar using rice husk char-supported nickel-iron catalysts for biomass pyrolysis/gasification. *Applied Catalysis B: Environmental*, 152-153, 140-151. DOI: 10.1016/j.apcatb.2014.01.032.

[40] Loy, A.C.M., Yusup, S., Chin, B.L.F., Gan, D.K.W., Shahbaz, M., Acda, M.N., Unrean, P., Rianawati, E. (2018). Comparative study of in-situ catalytic pyrolysis of rice husk for syngas production: Kinetics modelling and product gas analysis. *Journal of Cleaner Production*, 197, 1231-1243. DOI: 10.1016/j.jclepro.2018.06.245.

[41] Yang, H., Yan, R., Chen, H., Lee, D.H., Zheng, C. (2007). Characteristics of hemicellulose, cellulose and lignin pyrolysis. *Fuel*, 86, 1781-1788. DOI: 10.1016/ j.fuel.2006.12.013

[42] Lim, J.S., Manan, Z.A., Wan Alwi, S.R., Hashim, H. (2012). A review on utilisation of biomass from rice industry as a source of renewable energy. *Renewable and Sustainable Energy Reviews*, 16, 3084-3094. DOI: 10.1016/j.rser.2012.02.051

[43] Widiyannita, A.M., Pradana, Y.S., Cahyono, R.B., Sutijan, Akiyama, T., Budiman, A. (2020). Kinetic Study of Pyrolysis of Ulin Wood Residue using Thermogravimetric Analysis. International Journal on Advanced Science, *Engineering and Information Technology*, 10(4), 1624-1630; http://insightsociety.org/ojaseit/index.php/ijaseit/ article/view/3640

[44] Zhang, X., de Jong, W., Preto, F. (2009). Estimating kinetic parameters in TGA using B-spline smoothing and the Friedman method. *Biomass and Bioenergy*, 33, 1435-1441. DOI: 10.1016/j.biombioe.2009.06.009.

[45] Mishra, R.K., Mohanty, K. (2018). Pyrolysis kinetics and thermal behavior of waste sawdust biomass using thermogravimetric analysis. *Bioresource Technology*, 251, 63-74. DOI: 10.1016/j.biortech.2017.12.029.

[46] Orfao, J.J.M., Antunes, F.J.A., Figueiredo, J.L. (1999). Pyrolysis kinetics of lignocellulosic materials - three independent reactions model. *Fuel*, 78, 349-358. DOI: 10.1016/S0016-2361(98)00156-2.

[47] Sunarno, Rochmadi, Mulyono, P., Aziz, M., Budiman, A. (2017). Kinetic Study of Catalytic Cracking of Bio-oil over Silica-alumina Catalyst. *BioResources*, 13(1), 1917-1929. DOI: 10.15376/biores.13.1.1917-1929.

[48] Jamilatun, S., Budhijanto, Rochmadi, Yuliestyan, A., Hadiyanto, Budiman, A. (2019). Comparative Analysis Between Pyrolysis Products of Spirulina platensis Biomass and Its Residues. *International Journal of Renewable Energy Development*, 8(2), 133-140. DOI: 10.14710/ijred.8.2.133-140.

[49] Soleimanikutanaei, S., Ghasemisahebi, E., Lin, C.X. (2018). Numerical study of heat transfer enhancement using transverse microchannels in a heat sink. *International Journal of Thermal Sciences*, 125, 89-100. DOI: 10.1016/j.ijthermalsci.2017.11.009

[50] Nguyen, H.T., Gallardo, S.M., Bacani, F., Hinode, H., Minh Do, Q., Promentilla, M.A. (2015). Evaluating thermal properties of geopolymer produced from Red Mud, Rice Husk Ash and Diatomaceous Earth. *ASEAN Engineering Journal Part B*, 4(1), 51-65. DOI: 10.11113/aej.v4.15427

[51] Sotelo, C.D.R. (2018). Heat and mass transfer limitations in the pyrolysis of wood particles. *Thesis report*. Chemical Engineering – School of Engineering Sciences in Chemistry, Biotechnology and Health, Sweden.

[52] Jamilatun, S., Budhijanto, Rochmadi, Budiman, A. (2017). Noncatalytic Slow Pyrolysis of Sprulina Plantesis Residue for Production of Liquid Biofuel. *International Journal of Renewable Energy Development*, 7(4), 1901-1908. DOI: 10.20508/ijrer.v7i4.6305.g7233.

[53] Fu, Y., Zhang, N., Shen, Y., Ge, X., Chen, M. (2018). Micro-mesoporous carbons from original and pelletized rice husk via one-step catalytic pyrolysis. *Bioresource Technology*, 269, 67-73. DOI: 10.1016/j.biortech.2018.08.083.

[54] Uddin, M.J., Khan, M.M.R., Iftekhar, M.S., Islam, M.A. (2006). Cr(VI) removal from wastewater by using rice husk ash (RHA). *ASEAN Journal of Chemical Engineering*, 6(1), 53-57. DOI: 10.22146/AJCHE.50154

[55] Ahmaruzzaman, M., Gupta, V.K. (2011). Rice husk and its ash as low-cost adsorbents in water and wastewater treatment. *Industrial & Engineering Chemistry Research*, 50, 13589-13613. DOI: 10.1021/ie201477c

[56] El-Said, A.G., Badawy, N.A., Garamon, S.E. (2018). Adsorption of Heavy Metal Ions from Aqueous Solutions onto Rice Husk Ash Low Cost Adsorbent. *Journal of Environmental & Analytical Toxicology*, 8(1), 1000543. DOI: 10.4172/2161-0525.1000543